archaeometry

Archaeometry ••, •• (2017) ••–•• doi: 10.1111/arcm.12280

THE GLAZE TECHNOLOGY OF HISPANO-MORESQUE CERAMIC TILES: A COMPARISON BETWEEN PORTUGUESE AND SPANISH COLLECTIONS*

S. COENTRO[1]†, L. C. ALVES[2], C. RELVAS[3], T. FERREIRA[3], J. MIRÃO[4], J. MOLERA[5], T. PRADELL[6], R. A. A. TRINDADE[7], R. C. DA SILVA[8] and V. S. F. MURALHA[1] ‡

[1]*VICARTE—Research Unit 'Glass and Ceramic for the Arts', Faculdade de Ciências e Tecnologia, Universidade Nova de Lisboa, 2829-516 Caparica, Portugal*
[2]*C2TN-IST/UL, Centro de Ciências e Tecnologia Nucleares, Instituto Superior Técnico, Universidade de Lisboa, Estrada Nacional 10, 2695-066 Bobadela, Portugal*
[3]*Departamento de Química, Laboratório HERCULES, Escola de Ciência e Tecnologia, Universidade de Évora, Largo Marquês de Marialva, 8, 7000-809 Évora, Portugal*
[4]*Departamento de Geociências, Laboratório HERCULES, Escola de Ciência e Tecnologia, Universidade de Évora, Largo Marquês de Marialva, 8, 7000-809 Évora, Portugal*
[5]*MECAMAT, U Science Tech, University of Vic—Central University of Catalonia, C. de la Laura 13, 08500 Vic, Spain*
[6]*Departament de Física i Enginyeria Nuclear, Universitat Politècnica de Catalunya, Esteve Terradas 8, 08860 Castelldefels, Spain*
[7]*Museu Nacional de Arte Antiga (MNAA), Rua das Janelas Verdes, 1249-017 Lisboa, Portugal*
[8]*IPFN-IST/UL, Instituto de Plasmas e Fusão Nuclear, Instituto Superior Técnico, Universidade de Lisboa, Estrada Nacional 10, 2695-066 Bobadela, Portugal*

For the first time, Hispano-Moresque glazed tiles from Portuguese and Spanish collections were studied together and compared. This work is included in a wider study tackling the technology of Hispano-Moresque tile production from several collections in the Iberian Peninsula. While showing many similarities, differences were identified between collections, regarding both chemical and morphological characteristics. The collection from the Mosteiro de Santa Clara-a-Velha (Coimbra) stands out from the other collections, with higher SnO_2 content (up to 14 wt%), the highest Fe_2O_3 contents in amber glazes and a Ca-rich interface layer (mostly comprised of wollastonite, $CaSiO_3$). Samples from Palácio Nacional de Sintra (near Lisbon) and Seville-attributed samples (from the Instituto Valencia de Don Juan) are chemically similar, except that most Sintra's samples display a K-rich glaze/ceramic interface, whereas the ones from Seville exhibit both K-rich and Ca-rich inclusions. The samples attributed to Toledo show glazes with many inclusions, contrasting with the homogeneous glazes in most Hispano-Moresque tiles. From these results, we identify differences that can be used as markers in future studies on Hispano-Moresque tiles.

KEYWORDS: HISPANO-MORESQUE TILES, LEAD–TIN GLAZES, μ-PIXE, SR-μ-XRD, SEM–EDS

---

*Received 21 August 2015; accepted 29 July 2016
†Corresponding author: email scoentro@campus.fct.unl.pt
‡*In memoriam* our co-author and dear friend V. S. F. Muralha.
© 2017 University of Oxford

INTRODUCTION

Hispano-Moresque ceramic tiles

The *azulejo* (glazed tile) is the highlight of Portuguese cultural heritage, renowned after the second half of the 16th century, when the relevant works that embody the Portuguese *azulejo* production begun. Nevertheless, the designated Hispano-Moresque or medieval tiles were widely used in Portugal from the 15th century to the first half of the 16th century. Historically, this part of our cultural heritage has been considered to be imported from Spanish production centres, namely Seville, which by then was the main production centre in the Iberian Peninsula. There are indeed records of import orders to the Portuguese territory (Coimbra and Sesimbra), but archaeological evidence has shown that *arista* tiles were made in Portugal, near Barreiro, on the south bank of the Tagus River (Barros *et al.* 1999; Trindade 2007; Vieira Ferreira *et al.* 2014). Therefore, this subject is not consensual in our historical panorama and, recently, an analytical study has begun, aiming to contribute to settling this issue.

In order to clarify this key issue in tile manufacture from the Iberian Peninsula, it is important to analyse and compare data from Spanish and Portuguese collections. As far as we know, this is the first study comparing the chemical, mineralogical and morphological characterization of both Portuguese and Spanish collections of Hispano-Moresque architectural tiles. In a previous publication (Coentro *et al.* 2014), an important Portuguese collection was studied—the collection of the Mosteiro de Santa Clara-a-Velha, in Coimbra, Portugal. Those results are now compared with new data on tiles from Palácio Nacional de Sintra (Portugal) and on Spanish samples from the Instituto Valencia de Don Juan (Madrid) attributed to Seville and Toledo.

Hispano-Moresque tiles combine the technology of both tin-opacified glazes (usually for the whites and blues, but occasionally also for other colours) and transparent lead glazes. The production technology for these types of architectural decoration was inherited from the Muslims who occupied the Iberian Peninsula from the late eighth century AD onwards. It was adopted, developed and also simplified in Moresque workshops (Molera *et al.* 1997, 2009; Ortega *et al.* 2012).

The glaze technology used in Hispano-Moresque tiles was the focus of this study: glaze compositions, colours and morphologies provide important information with which to compare production centres and contextualize tile production in the ceramics manufacture throughout the Iberian Peninsula.

Collections

The Palácio Nacional de Sintra (PNS) has stood since at least the 13th century, but most of its Hispano-Moresque decorations belong to the reign of King Manuel I (1495–1521). By the end of the 15th century, major construction works had taken place in the palace and thousands of Hispano-Moresque tiles were being used to decorate its walls. It is usually said that the tiles came from Seville and were unloaded at the Belém seaport, in Lisbon. This idea is still subject to debate, since the document referring to tiles in Belém does not mention their origin, and there are very unusual motifs in the PNS collection, unknown anywhere else in the world, such as the armillary sphere and some relief tiles with wine-related motifs (Trindade 2007). Furthermore, it is now known that there was production of Hispano-Moresque tiles on the south bank of the Tagus River, as previously mentioned.

The Mosteiro de Santa Clara-a-Velha (SCV) was founded in 1283 and definitely abandoned in 1677. Located on the left bank of the Mondego River, just opposite ancient Coimbra, the building suffered from constant floods, which ultimately led to the construction of a new Santa Clara

Monastery, on a higher location nearby (Côrte-Real *et al.* 2010). The church and cloister, which are now ruins, have been partially restored and opened to the public. Over recent decades, several archaeological campaigns have uncovered an extraordinary Hispano-Moresque tile collection, including a variety of patterns and production techniques (*arista*, *cuerda seca*, relief and flat tiles).

The Instituto Valencia de Don Juan (IVDJ) is located in Madrid, Spain. It was founded in 1916 to host the collection of decorative arts and documents that comprises one of the most important sets of Hispano-Moresque ceramics in the world, including tiles from Seville, Toledo and Valencia. Its founders were the owners of such collections: Don Guillermo de Osma y Scull and his wife Doña Adelaida Crooke y Guzmán (XIII Condesa de Valencia de Don Juan).

EXPERIMENTAL PROCEDURE

Samples

Cross-section samples (1–2 mm wide) from the collections of the PNS and the IVDJ were collected and mounted in epoxy resin (Araldite® 2020). They were all polished on Micro-Mesh® sheets up to grit 8000. μ-PIXE, μ-Raman and SEM–EDS analyses were performed on these polished cross-section samples. Only μ-XRD analysis required thin-cut polished cross-sections, as explained below.

The results were compared with those from our previous publication on the collection of the SCV (Coentro *et al.* 2014). In total, 70 samples were studied (each one of them comprising several coloured glazes): 30 from the PNS collection, 19 from the SCV collection and 21 from the IVDJ collection. In the latter set, there are samples attributed to Toledo and to Seville, indicated as IVDJ-T and IVDJ-S, respectively, in the tables and figures. A tile from each collection is represented in Figure S1.

Analytical techniques

μ-PIXE Particle-induced X-ray emission with micrometre lateral resolution (μ-PIXE) was performed using an Oxford Microbeams OM150 type scanning microprobe capable both of focusing the 1 MeV proton beam that was used down to $3 \times 4\ \mu m^2$ and scanning a sample surface area as large as $3730 \times 3730\ \mu m^2$. The sample fragments were irradiated in vacuum and a $30\ mm^2$ Bruker SDD with 145 eV resolution was used for X-ray collection. Equipped with an 8 μm thick Be window, it allows the detection of X-ray energies as low as those of Na, while preventing most of the protons from entering and damaging the detector crystal. From the initially obtained 2D elemental distribution maps (with typical dimensions of $750 \times 750\ \mu m^2$), the glaze and the ceramic body of the tiles could be properly identified and a representative region of interest selected for quantitative analysis. Operation and basic data manipulation was achieved through the OMDAQ software code (Grime and Dawson 1995), while quantitative analysis was performed with the GUPIX code (Campbell *et al.* 2010). In order to validate the results, two glass reference standards (Corning Museum of Glass B and C) were also analysed (Table 1).

SEM–EDS The equipment used for the analyses was a HITACHI S-3700 N variable-pressure scanning electron microscope coupled with a Bruker Xflash 5010 SDD energy-dispersive X-ray spectrometer. Samples were analysed either in vacuum (in which case the samples were coated with a thin, conductive film of carbon), or under an air pressure of 20 Pa or 40 Pa (with uncoated samples). The backscattering mode was used for SEM imaging. The resolution of the EDS

Table 1 *µ-PIXE values obtained for the glass standards Corning Museum of Glass (CMoG) B and C: certified values obtained from Brill (1999)*

Glass standards	Na_2O	MgO	Al_2O_3	SiO_2	K_2O	CaO	TiO_2	MnO	Fe_2O_3	CoO	NiO	CuO	BaO	PbO
CMoG B														
Certified (wt%)	17	1.03	4.36	62.27	1	8.56	0.089	0.25	0.34	0.046	0.099	2.66	0.12	0.61
Measured (wt%)	17.1	0.96	4.3	64.8	0.96	7.5	0.12	0.22	0.30	0.08	0.10	2.3	0.10	0.43
SD* (wt%)	1.2	0.05	0.3	1.0	0.05	0.4	0.02	0.04	0.03	0.03	0.02	0.2	0.04	0.13
CMoG C														
Certified (wt%)	1.07	2.76	0.87	34.3	2.84	5.07	0.79	–	0.34	0.18	–	1.13	11.4	36.7
Measured (wt%)	1.14	2.4	0.89	35.8	2.60	4.42	0.6	–	0.30	0.16	–	1.09	11.5	38.8
SD (wt%)	0.09	0.1	0.04	1.3	0.06	0.08	0.1		0.02	0.03		0.06	0.2	1.8

*SD, standard deviation.

detector is 123 eV at the Mn–K_α line energy. The system allows reliable chemical point analysis and mapping from Na–K_α X-ray emission energy up to the L emissions of the heaviest elements. In order to collect X-ray emissions from heavier elements such as Pb, an acceleration voltage of 20 kV was chosen. The EDS tasks and the quantification were achieved through the Esprit 1.9 software package, from the Bruker Corporation.

μ-Raman Analyses were performed using a Labram 300 Jobin Yvon spectrometer, equipped with a He–Ne laser of 17 mW power operating at 633 nm and a solid state laser of 500 mW power operating at 532 nm. The laser beam was focused either with 50× or 100× Olympus objective lenses. The laser power was filtered to 10% incident power using a neutral density filter for all analyses. Analyses were performed both on the surface of the glazes and on polished cross-sections. Spectra were recorded as an extended scan. A mixed Gaussian–Lorentzian curve-fit provided by the LabSpec software (v. 5.15.25) was used to determine the exact peak wavenumbers. The attribution of the Raman spectra was made using the RRUFF database project on minerals (RRUFF 2014).

μ-Diffraction Analyses were performed in the Material Science Powder Diffraction (MSPD) beamline at the Spanish synchrotron ALBA-CELLS. Small fragments (a few mm) of eight samples from the PNS, SCV and IVDJ collections were embedded in an epoxy resin and fixed on to a glass microscope slide. Thin sections of thickness 30 μm were obtained by grinding by hand and samples were polished with 1 μm diamond paste in order to be studied under the petrographic microscope. Using a polished thin cut, it is also possible to study the nature and spatial distribution of the crystalline compounds by microscopy, and the same thin section is used for μ-diffraction analyses. Micro-X-ray diffraction with synchrotron radiation (SR-μ-XRD) was performed using a wavelength of 0.04133 nm (30 keV) and a spot size of 20 × 20 μm, and was recorded using a SX165 Rayonix CCD detector.

RESULTS AND DISCUSSION

The ceramic body of the tiles is briefly described here, as this study is focused on the glazes. μ-PIXE analysis performed on the ceramic bodies revealed similar compositions in most samples, with a Ca-rich composition (~15–25 wt% CaO) consistent with the creamy-pink colour range. The main constituent oxides are SiO_2, CaO, Al_2O_3, Fe_2O_3, MgO and K_2O, with SiO_2 values between 47 wt% and 60 wt% and Al_2O_3 contents in the 11–17 wt% range. The IVDJ-T samples stand out for their orange ceramic bodies, although quantitative analysis did not reveal considerable differences when compared to the other collections. Higher hematite (Fe_2O_3) contents may explain the orange hues, whereas in the SCV, PNS and IVDJ-S samples the iron ions may have been incorporated in pyroxenes and other phases that form at 900–950 °C (Molera *et al.* 1998). These differences will be addressed in a separate study yet to be published.

All of the samples in this study were decorated with glazes of the same five colours—white, blue, green, amber and brown—which look similar by visual inspection amongst all groups. However, different shades were identified and will be discussed separately for each colour.

Microprobe PIXE X-ray mapping and point analysis showed the occurrence of elemental distributions of Sn, Co, Cu, Fe and Mn—elements known to confer colours in glazes—in tight correlation with the glazes colours: white (SnO_2), blue (SnO_2 and CoO), green (CuO), amber (Fe_2O_3) and brown (MnO). At the macroscopic and mesoscopic levels, the colours are very homogeneous, while no particles or inclusions were identified by SEM–EDS or μ-Raman that would suggest a particular raw material.

Content analysis for the PNS, SCV and IVDJ samples, obtained through quantitative μ-PIXE, are presented in summarized form in Table 2. Detailed quantification results for each sample may be found in Table S1 (samples that were previously analysed in Coentro *et al.* 2014 are indicated accordingly). SiO_2 and PbO are the major constituents of the glazes, making up to 90 wt% of the total composition. They show an inverse correlation (Fig. 1 (a)), with lower SiO_2/PbO ratios for the majority of green, brown and amber glazes than for the white and blue ones.

The chemical composition of the majority of glazes (namely in *arista* and *cuerda seca* tiles) can be divided in two groups according to their SnO_2 content (Fig. 1 (b)), with blue and white glazes having higher SnO_2 contents on one side (~4–14 wt%), and most green, amber and brown glazes having lower values (~0–3 wt% SnO_2).

However, there are exceptions in the IVDJ and, in particular, the PNS collection, namely with some green and brown glazes having higher SnO_2 contents. In the PNS collection, these exceptions correspond to relief tiles, where, according to chemical analysis, a white tin glaze seems to be the base recipe for all colours.

Glaze analysis by colour

White and blue glazes PIXE characterization showed that tin oxide is the third major constituent in the white and blue glazes for all three collections under study and is also one distinguishing factor amongst these collections, with higher SnO_2 contents in the white and blue glazes of the SCV collection (~7–14 wt%). Figure 1 (c) shows how the SCV collection stands out from the others, with a larger spread and a tendency towards higher SnO_2/PbO wt% ratios for most white and blue samples.

The PNS collection tiles have SnO_2 contents that do not exceed 9 wt% (except for a flat monochromatic white sample, PNS04, which contains 12 wt% SnO_2). The IVDJ-S samples show higher amounts of SnO_2 (5–11 wt%) than the IVDJ-T ones (4–8 wt%).

Figure 1 (b) shows that a higher Na_2O content is associated with tin-opacified glazes, which suggests that a sodium compound could have been intentionally added, perhaps as a flux to compensate for the lower PbO contents.

When comparing with published data on coeval tin glazes, the results obtained for tin oxide contents in the PNS and IVDJ collections agree with those for Hispano-Moresque white glazes analysed by several authors (Molera *et al.* 1997, 2001a; Pérez-Arantegui *et al.* 2005, 2009; Chabanne *et al.* 2008; Vieira Ferreira *et al.* 2014). However, higher tin oxide contents, such as those found in SCV samples, are not common in any type of known Hispano-Moresque ceramics and have only been measured in Islamic white-glazed ceramics from Zaragoza and Córdoba (Molera *et al.* 2001a). The lack of specific studies on Hispano-Moresque tiles does not yet allow us to determine if this is a particular characteristic of the SCV tiles or if high SnO_2 contents were used in more tile collections throughout the Iberian Peninsula.

The Fe_2O_3 contents in the white glazes are mostly inferior to 1 wt%, which could mean that the raw materials underwent some kind of purification process, or that a high-quality sand was used, which was low in impurities (Pérez-Arantegui *et al.* 2005, 2009).

Cross-sectional SEM shows that the large majority of Hispano-Moresque tiles in this study have very homogeneous tin-opacified glazes, with few mineral inclusions (mostly quartz and potassium feldspars, as discussed below) and gas bubbles (Figs 2 (a) – 2 (c)). Tin oxide is easily observed in every blue or white glaze, and also in some green and brown tin-opacified glazes, as

Table 2 *The average chemical composition (in wt%) of the analysed tiles from the PNS, SCV and IVDJ collections, obtained by μ-PIXE: the results are divided by colour and technique (A, arista; CS, cuerda seca; R, relief; F, flat)*

	Technique	*Na_2O*	*MgO*	*Al_2O_3*	*SiO_2*	*Cl*	*K_2O*	*CaO*	*TiO_2*	*MnO*	*Fe_2O_3*	*CoO*	*NiO*	*CuO*	*SnO_2*	*BaO*	*PbO*
White glaze																	
PNS	F (PNS 04)	1.49	0.29	0.42	29.2	0.98	0.21	0.28			0.21				11.65		55.3
	CS (*n* = 9)	2.35	0.51	1.87	40.8	0.76	2.72	1.97	0.12		0.47			0.15	6.90		41.5
	±	0.46	0.14	0.52	2.7	0.15	0.83	0.51	0.03		0.15			0.05	1.13		3.8
	R (*n* = 10)	2.41	0.46	1.69	40.2	0.82	2.75	2.08	0.14	0.11	0.46			0.18	7.48		41.5
	±	0.61	0.21	0.54	4.3	0.36	0.53	0.95	0.06	0.05	0.20			0.09	0.68		5.3
	A (*n* = 6)	2.55	0.61	2.57	44.0	0.70	2.24	2.63	0.15		0.63				6.26		37.7
	±	0.24	0.17	0.64	2.4	0.28	0.90	0.73	0.03		0.15				1.15		3.6
SCV	CS (*n* = 7)	2.22	0.71	2.48	45.2	0.38	2.78	2.34	0.14	0.04	0.65			0.12	8.13		34.9
	±	0.62	0.25	1.06	3.9	0.15	0.78	0.66	0.03	0.01	0.18			0.06	2.67		6.0
	A (*n* = 7)	2.11	0.89	2.71	43.6	0.37	2.65	2.51	0.13		0.65			0.28	9.13		35.1
	±	0.50	0.55	0.25	4.1	0.18	0.99	1.13	0.06		0.29			0.25	2.95		4.3
IVDJ-S	CS (*n* = 8)	2.43	0.50	2.42	40.2	0.59	1.93	2.12	0.12	0.09	0.52			0.08	7.15		42.0
	±	0.61	0.15	1.14	4.2	0.32	0.90	0.87	0.04	0.05	0.17			0.01	1.98		5.3
	A (*n* = 5)	2.44	0.79	2.88	42.2	0.28	2.23	3.27	0.13		0.64			0.06	7.78		37.3
	±	0.65	0.20	0.68	3.3	0.12	0.95	1.51	0.04		0.16			0.02	1.37		4.6
IVDJ-T	A (IVDJ-T 133)	0.97	0.42	4.27	47.9	0.22	1.66	0.96	0.08		0.41			0.05	5.99		37.0
	A (IVDJ-T 3683)	0.73	0.61	3.59	45.2	0.30	2.12	1.70	0.08		0.31				8.05		37.3
Blue glaze																	
PNS	F (PNS 01)	3.16	0.41	1.61	35.6	0.58	2.20	1.73	0.11	0.09	1.77	0.43	0.19	0.24	7.67		44.2
	CS (*n* = 7)	2.59	0.50	2.14	42.8	0.81	3.09	2.46	0.12	0.04	1.47	0.37	0.20	0.25	6.20		36.7
	±	0.51	0.10	0.49	2.8	0.29	1.02	0.61	0.02	0.01	0.20	0.06	0.09	0.11	0.78		3.8
	R (*n* = 3)	2.60	0.57	2.13	40.1	0.43	3.04	2.94	0.15	0.09	1.84	0.38	0.18	0.33	7.17		38.0
	±	0.34	0.14	0.37	3.5	0.01	0.73	0.71	0.03	0.08	0.17	0.04	0.03	0.11	1.22		3.4
	A (*n* = 6)	2.42	0.72	2.34	44.0	0.55	2.14	2.70	0.13		1.26	0.33	0.16	0.15	5.92		36.2
	±	0.37	0.14	0.48	4.0	0.19	0.65	0.73	0.02		0.53	0.12	0.08	0.06	1.25		4.3
SCV	F (SCV 86i4886)	2.53	0.72	2.22	43.2	0.35	3.73	3.15	0.12	0.02	2.09	0.42	0.11	0.05	11.27		29.7
	CS (*n* = 6)	2.64	0.58	2.07	43.2	0.38	2.45	2.14	0.18	0.04	1.34	0.33	0.18	0.31	9.45		34.7
	±	0.59	0.12	0.45	2.8	0.32	0.51	0.29	0.11	0.02	0.44	0.14	0.06	0.11	5.05		4.4
	R (SCV 14CF2686)	2.01	0.78	2.19	39.4	0.23	1.97	2.65	0.15		1.51	0.30	0.21	0.45	12.56		35.6

(*Continues*)

Table 2 *(Continued)*

	Technique	Na_2O	MgO	Al_2O_3	SiO_2	Cl	K_2O	CaO	TiO_2	MnO	Fe_2O_3	CoO	NiO	CuO	SnO_2	BaO	PbO
	A ($n = 9$)	2.35	0.67	2.24	41.6	0.33	2.68	2.70	0.14	0.06	1.76	0.44	0.19	0.34	9.29		35.2
	±	0.36	0.10	0.33	1.6	0.14	0.74	0.44	0.02	0.05	0.33	0.09	0.04	0.26	2.70		3.5
IVDJ-S	CS ($n = 4$)	3.10	0.42	2.13	41.9	0.66	2.35	2.01	0.11	0.04	1.61	0.45	0.20	0.25	6.01		38.8
	±	0.28	0.17	0.48	2.8	0.18	0.71	0.74	0.02	0.01	0.42	0.15	0.07	0.10	0.86		4.9
	A ($n = 8$)	2.83	0.80	3.00	41.8	0.46	2.56	3.03	0.16	0.05	2.31	0.64	0.27	0.32	7.06		34.8
	±	0.72	0.37	0.86	2.7	0.32	0.98	1.67	0.04	0.02	1.12	0.39	0.18	0.31	1.38		6.3
IVDJ-T	A ($n = 3$)	2.09	0.72	3.86	42.8	0.68	2.11	1.70	0.10	0.06	1.03	0.29	0.15	0.22	4.95		39.6
	±	2.27	0.30	0.57	3.1	0.52	0.87	1.09	0.01	0.08	0.57	0.03	0.03	0.13	1.31		6.0
Green glaze																	
PNS	F (PNS 02)	1.17	0.69	3.03	38.6	0.21	2.01	3.38	0.18		0.80			1.94	1.26		46.8
	F (PNS 03)	1.00	0.12	0.57	32.9	0.36	0.30	0.37			0.27			2.98	7.17		54.0
	CS ($n = 6$)	1.53	0.48	2.78	40.7	0.33	2.42	2.44	0.21	0.17	0.90			1.68	2.23		44.3
	±	0.18	0.18	0.81	2.8	0.06	0.73	0.83	0.10	0.17	0.29			0.50	0.97		4.4
	R ($n = 6$)	1.57	0.46	1.93	36.3	0.48	1.91	2.57	0.12		0.77			2.99	2.93		48.1
	±	0.91	0.10	0.48	2.2	0.18	0.75	0.49	0.06		0.11			1.61	2.94		5.9
	A ($n = 5$)	0.90	0.44	2.29	37.5	0.24	1.40	2.60	0.15	0.08	0.88			1.84	1.08		51.0
	±	0.34	0.07	0.36	1.7	0.09	0.49	0.55	0.03	0.05	0.13			0.35	0.92		3.3
SCV	CS ($n = 3$)	1.26	0.74	2.67	39.9	0.27	1.98	2.84	0.16	0.11	0.95			2.66	1.84		45.3
	±	0.32	0.21	0.90	4.5	0.11	0.58	0.26	0.05	0.11	0.37			0.52	0.11		6.5
	A ($n = 5$)	1.38	1.01	3.40	41.2	0.27	2.33	3.88	0.19	0.07	0.96			2.09	1.40		42.2
	±	0.35	0.45	0.99	3.2	0.09	0.85	0.81	0.03	0.05	0.21			0.74	0.34		4.2
IVDJ-S	CS ($n = 8$)	1.69	0.46	2.17	39.0	0.36	1.67	1.94	0.14	0.02	0.57			2.19	3.44		46.4
	±	0.52	0.09	0.49	3.9	0.25	0.70	0.63	0.05	0.03	0.14			0.70	2.80		2.9
	R (IVDJ-S XV)	1.13	0.53	3.32	37.8	0.22	1.23	2.83	0.15		1.06			1.51	3.20		47.0
	A ($n = 3$)	2.23	0.69	3.06	42.3	0.40	2.56	2.95	0.16		0.97			1.38	4.58		40.4
	±	1.17	0.20	0.61	3.7	0.08	1.02	0.69	0.05		0.40			0.33	5.67		10.0
IVDJ-T	A (IVDJ-T 96)	1.01	0.91	3.76	35.6		1.62	2.90	0.24		0.68			2.66	3.77		44.9
	A (IVDJ-T 133)	0.59	0.66	3.75	42.9	0.17	1.07	1.38	0.10	0.02	0.55			1.22	0.62		46.9
Amber glaze																	
PNS	CS ($n = 3$)	1.01	0.56	2.20	38.3		2.52	1.91	0.16	0.13	3.90				0.75		48.6

(*Continues*)

Table 2 *(Continued)*

	Technique	*Na_2O*	*MgO*	*Al_2O_3*	*SiO_2*	*Cl*	*K_2O*	*CaO*	*TiO_2*	*MnO*	*Fe_2O_3*	*CoO*	*NiO*	*CuO*	*SnO_2*	*BaO*	*PbO*
	±	0.59	0.61	0.96	2.6		0.51	1.51	0.04	0.10	0.03				0.24		56.0
	R CS (PNS 14)	2.32	0.72	4.28	47.7	0.18	3.39	3.78	0.24	1.76	1.55			0.09	2.47		31.5
	R (PNS 15)	1.56	0.52	2.70	40.8		2.80	3.48	0.16		3.92			0.27	0.94		42.9
	A ($n = 5$)	0.78	0.58	2.56	37.4	0.21	1.63	3.09	0.17		3.60			0.14	0.49		49.5
	±	0.16	0.19	0.20	3.5	0.05	0.32	0.78	0.01		0.52			0.01	0.06		4.2
SCV	CS ($n = 6$)	1.37	0.68	2.87	39.3	0.32	2.76	3.20	0.19	0.14	4.29			0.08	3.28		43.4
	±	0.82	0.24	1.06	4.2	0.09	0.57	0.88	0.05	0.16	0.98			0.03	4.12		7.3
	A ($n = 5$)	1.34	0.80	3.11	36.0	0.28	2.26	3.85	0.20	0.03	4.31			0.15	0.76		47.0
	±	0.46	0.09	0.74	1.1	0.10	0.32	0.60	0.06	0.01	0.51			0.13	0.39		2.8
IVDJ-S	CS ($n = 3$)	0.94	0.47	2.03	38.5	0.23	1.89	1.93	0.15		3.89				0.59		49.5
	±	0.51	0.10	0.45	3.6	0.05	1.39	0.62	0.02		0.53				0.22		6.0
	A ($n = 3$)	1.34	0.72	3.12	41.5	0.21	2.22	3.22	0.19		3.47						44.0
	±	0.11	0.18	0.09	2.4	0.00	1.38	0.49	0.02		0.24						2.8
IVDJ-T	A ($n = 4$)	0.83	0.81	4.70	40.0	0.19	1.96	3.55	0.14	0.09	2.45				0.71	0.64	44.4
	±	0.17	0.22	1.20	8.0	0.09	0.66	1.68	0.03	0.04	0.38				0.36	0.07	9.0
Brown glaze																	
PNS	CS ($n = 5$)	1.03	0.37	2.10	37.7	0.27	2.36	2.08	0.16	3.45	1.13			0.15	0.59	0.15	48.7
	±	0.32	0.13	0.38	2.7	0.02	0.55	1.12	0.03	1.07	0.30			0.07	0.21	0.03	2.7
	R ($n = 5$)	2.01	0.58	2.34	39.0	0.54	3.34	2.65	0.13	1.76	0.92			0.25	6.61	0.22	40.0
	±	0.15	0.13	0.59	1.9	0.16	1.02	0.95	0.03	0.31	0.20			0.08	2.94	0.10	2.3
	A ($n = 3$)	1.00	0.71	2.80	40.6	0.25	1.92	3.46	0.19	2.26	1.16				0.65		45.1
	±	0.36	0.22	0.08	0.4	0.06	0.16	0.73	0.01	0.32	0.54				0.14		0.5
SCV	CS ($n = 6$)	1.61	0.86	3.54	41.1	0.23	2.98	3.47	0.20	5.00	2.20			0.18	1.07	0.33	37.3
	±	0.24	0.19	1.00	3.5	0.07	1.01	0.60	0.03	4.47	0.52			0.15	0.57	0.14	6.6
	A ($n = 4$)	1.23	0.88	3.01	40.0	0.26	2.62	3.49	0.18	2.68	1.98			0.55	0.93	0.24	42.5
	±	0.34	0.29	0.36	4.2	0.08	1.11	1.31	0.02	0.82	1.02			0.70	0.15	0.06	2.1
IVDJ-S	CS ($n = 5$)	0.94	0.45	2.01	38.5	0.26	1.07	1.78	0.15	3.26	0.88			0.08	0.82	0.17	50.1
	±	0.52	0.14	0.45	2.6	0.08	0.26	0.73	0.03	1.17	0.24				0.41	0.01	3.7
	A (IVDJ-S 3584)	1.33	1.22	4.22	43.2		1.51	5.00	0.24	2.76	1.73			0.12			38.7

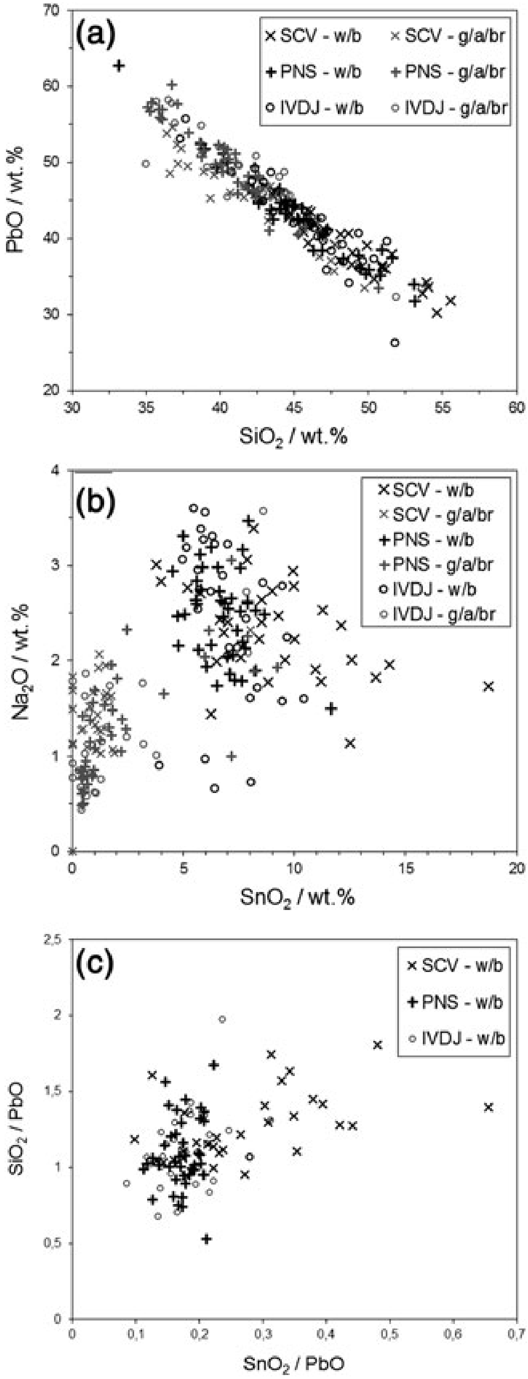

Figure 1 *Binary plots obtained through μ-PIXE analysis: (a)* SiO_2 *versus PbO (wt%), where an inverse correlation can be seen, with white and blue glazes showing higher* SiO_2 *and lower PbO contents; (b)* SnO_2 *versus* Na_2O *(wt%), where tin-opacified glazes (mostly white and blue) are associated with higher* Na_2O *contents; (c)* SnO_2/PbO *versus* SiO_2/PbO*, where SCV samples stand out for their higher* SnO_2/PbO *ratios.*

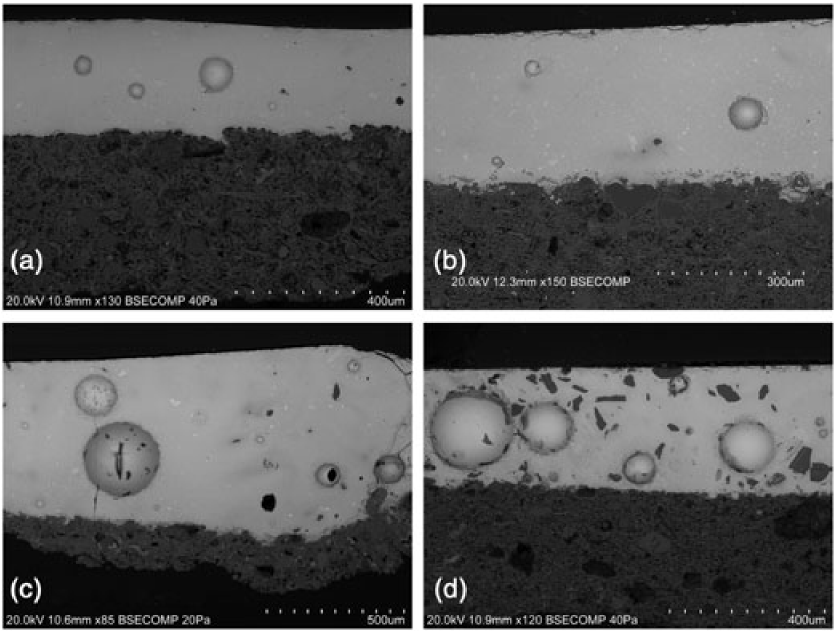

Figure 2 *BSE images of four white and blue glazes in cross-section: (a) PNS 23—white; (b) SCV 33Bi3839—blue; (c) IVDJ-S 3561—blue (attributed); (d) IVDJ-T 4095—blue (attributed).*

previously mentioned. Tin oxide particles appear in very small agglomerates. As suggested by previous results for SCV tiles (Coentro *et al.* 2014), the small size and homogeneous distribution of tin oxide crystals in PNS (Fig. 3) and IVDJ-S opaque glazes are consistent with a fritted glaze technology (Molera *et al.* 1997, 2001a; Vendrell-Saz *et al.* 2006).

The IVDJ-S samples show morphological similarities with Portuguese (SCV and PNS) collections (Figs 2 (a) – 2 (c)). However, the IVDJ-T samples show heterogeneous glazes, with mineral inclusions (mostly quartz) (Fig. 2 (d)). Such mineral inclusions were intentionally used in Hispano-Moresque white glazes from Teruel (Pérez-Arantegui *et al.* 2005, 2009), as they contribute to the opacification of the glaze and lower the production costs by reducing the necessary amount of tin.

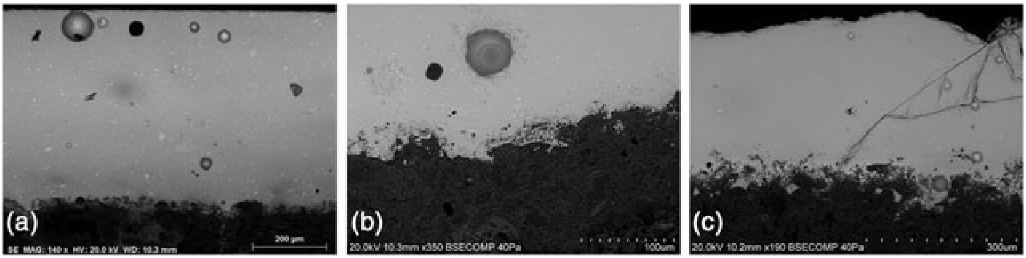

Figure 3 *BSE images of tin-opacified PNS glazes in cross-section: small tin oxide agglomerates homogeneously distributed throughout the white glaze of (a) a cuerda seca tile (PNS 19), and the (b) blue (PNS07) and (c) green (PNS09) glazes in relief tiles.*

Blue glazes, in particular, have shown a similar composition in all three collections, displaying a Fe–Co–Ni–Cu association. Some samples contain very low Mn contents as well. The Fe–Co–Ni–Cu association has also been identified for Italian and Spanish ceramics from the 14th–16th centuries (Roldán *et al.* 2006).

Although this association of elements was identified for all SCV samples (Coentro *et al.* 2012), there are other combinations in PNS blue glazes, in particular with the identification of As:

- Fe–Co–Ni–Cu–As (PNS20);
- Fe–Co–Ni–As (PNS22);
- Fe–Co–Ni–As–Bi (PNS29).

The presence of As in the blue pigment composition has been identified in glasses and glazes dated from the end of the 15th century onwards (Gratuze *et al.* 1997; Roldán *et al.* 2006; Zucchiatti *et al.* 2006). These differences in cobalt associations do not necessarily mean that the pigment was imported from more than one location, since all the above-mentioned cobalt associations existed in the mining district of Erzgebirge (Saxony), in Germany, which was the most important cobalt source at that time (Gratuze *et al.* 1997; Roldán *et al.* 2006; Zucchiatti *et al.* 2006). According to Zucchiatti *et al.* (2006), the presence of arsenic from the 16th century onwards could be associated with a change in the production of *zaffre* (calcinated cobalt ore, mixed with sand), which occurred in the Saxony region (Zucchiatti *et al.* 2006).

On the other hand, different sources for the cobalt pigment are still possible. The origin of the use of cobalt in the Iberian Peninsula derives from the Muslim occupation and dates back to at least the 13th century (Trindade 2007). Cobalt deposits were known in the Morocco and Persia regions, from where several ceramists journeyed to the Iberian Peninsula (Trindade 2007).

Green glazes Three main shades of green glazes were identified: a transparent dark green, an opaque tin-opacified green and a turquoise green. The SCV collection stands out for only containing the first type of green glaze.

The compositions of the green ‘transparent’ glazes identified in most *arista* and *cuerda seca* samples, from all three collections, were found to be comprised of 1–3 wt% CuO and <2 wt% SnO_2. This dark transparent type is the most common in Hispano-Moresque tiles.

The PNS and IVDJ collections contain tin-opacified green glazes, with SnO_2 contents between 3 wt% and 9 wt%. Glazes with SnO_2 values above 7 wt% exhibit a turquoise shade (PNS03, IVDJ 3561, 3794 and 3919), which is easily differentiated from the common dark green in the other tiles. Other tin-opacified greens with 3–4 wt% SnO_2 were found in Spanish samples and a *cuerda seca* PNS tile (PNS06, the armillary sphere).

In IVDJ 3561, turquoise glaze—malayaite $CaSnO(SiO_4)$—was identified by both synchrotron μ-XRD (Fig. 4) and μ-Raman (Fig. 5 (a)). Malayaite had previously also been identified in two SCV green glazes (Coentro *et al.* 2014). This calcium–tin silicate is formed through a reaction between the calcium and the tin in the glaze melt (Mulholland 1984).

Amber glazes In amber glazes, high Fe_2O_3 contents (2–5 wt%) were identified. When compared to the other colours, the Fe_2O_3/SiO_2 ratio is considerably higher in amber glazes, which suggests the intentional addition of Fe compounds to obtain the colour.

The highest Fe_2O_3 contents, mostly above 4 wt%, are observed in the SCV collection, whereas in the PNS and IVDJ amber glazes, Fe_2O_3 is almost always below this value. However, it is known that the chemical composition of the glaze is influenced by the reaction that occurs with the ceramic body during firing (Molera *et al.* 2001b). Thus, small differences in clay constituent

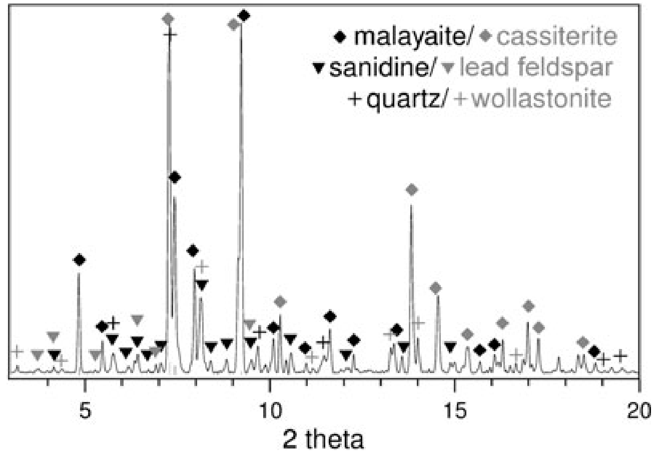

Figure 4 *A diffractrogram of turquoise green glaze, near the interface of sample IVDJ 3561-S, where malayaite, cassiterite, sanidine/lead feldspar, quartz and wollastonite were identified.*

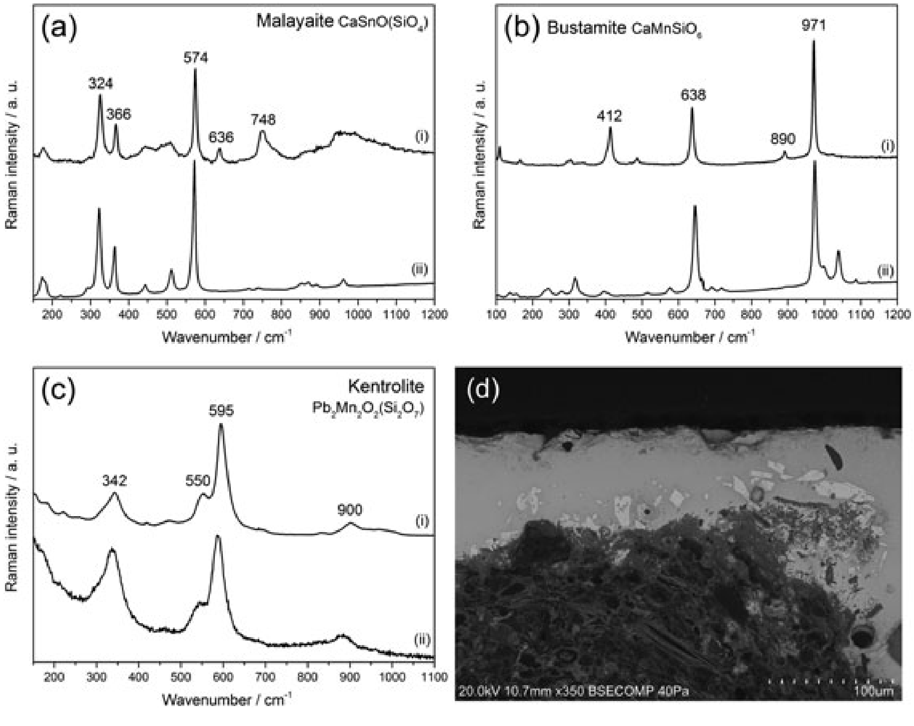

Figure 5 *The µ-Raman spectra of (a) malayaite—(i) IVDJ-S 3561 and (ii) the reference spectrum; (b) bustamite—(i) PNS07 and (ii) the reference spectrum; (c) kentrolite—(i) IVDJ 4095-T and (ii) the reference spectrum. (d) The BSE image shows kentrolite crystals in the brown glaze of sample 4095-TL: these crystals appear whiter due to Pb in their composition.*

oxides such as Al_2O_3, CaO and Fe_2O_3 can be related to the ceramic body composition and firing conditions, instead of a different glaze recipe.

Brown glazes Brown manganese glazes appear as a dark colour with various shades, sometimes also referred to as 'purple' or 'black'.

In PNS relief tiles, manganese was mixed with a white tin glaze, which results in an opaque lighter colour that is unique in this collection, and in this group of tiles in particular. It is a different shade from the one observed in later majolica tiles, where the manganese pigment was applied on the glaze with a brush. In the PNS relief tiles, manganese brown is a homogeneous colour.

The brown glazes display MnO contents between 2 wt% and 5 wt%. Manganese appears associated with higher iron contents. Barium also appears associated with manganese in approximately half of the samples, is frequent in manganese-brown decorations (Coentro *et al.* 2012, 2014; Molera *et al.* 2013) and has been attributed to the Ba-containing minerals (Ba-feldspars, psilomelane $(Ba,H_2O)_2Mn_5O_{10}$) and barite $BaSO_4$) that are abundant in manganese ore sources (Tite *et al.* 2009).

Analysis of the glaze/ceramic interface Figure 6 illustrates the typical glaze and glaze/ceramic interface found in white and blue glazes. In the PNS samples, the interface is generally thinner (~30–70 μm) than in the SCV samples (~30–100 μm)—the interface thickness is considered here as the layer with mineral inclusions that results from the reaction between the glaze and the ceramic body of the tile. Thicker interfaces (up to 100 μm) are visible in brown and amber glazes in all collections. When there is a stronger reaction between the glaze and the ceramic body, this initiates a large number of small mineral inclusions that are spread through the glaze until they reach the surface. The interface thickness can be an indicator of the firing technology, namely the number of firings. According to Molera *et al.* (2001b), a single-fired object will present thicker interfaces (>30 μm) than a double-fired one (~10 μm), due to the reaction between glaze

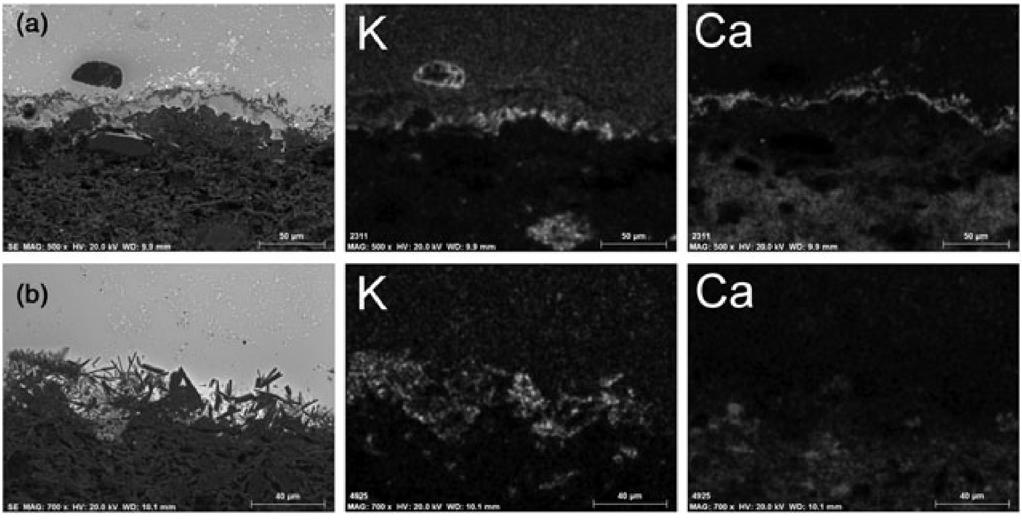

Figure 6 *EDS X-ray maps, comparing the (a) SCV (SCV 45 M4260—white) and (b) PNS (PNS09—white) glaze/ceramic interfaces. A Ca-rich layer, absent in the PNS sample (b), is observed in the SCV one (a).*

and ceramic body, which is stronger when the latter is unfired. Studies on Islamic and Hispano-Moresque lead-glazed ceramics have indicated that a double-firing process was used in Islamic workshops, but it was progressively abandoned in Hispano-Moresque ones, as suggested by the study of 14th–15th century ceramic fragments from workshops in Paterna (Molera *et al.* 1997). However, Hispano-Moresque tin-glazed ceramics from Teruel, Spain, and also every coeval lustre-decorated ceramic from several Iberian production centres exhibit thinner interfaces ($< 10\,\mu m$), consistent with the continuity of a double-firing process (Molera *et al.* 1997, 2001b; Pérez-Arantegui *et al.* 2005, 2009), but in these cases tiles exhibit a thicker glaze than tin-glazed wares, and thicker glazes develop thinner interfaces in single firing. In the particular case of Hispano-Moresque tiles, the results do not allow us to determine whether one or two firings took place, as more data is needed for the tin-glazed ceramics. It is also possible that the ceramic body was previously fired at a low temperature, or that a slip was used to increase the adherence of the glaze on the ceramic substrate.

Chemical and phase analysis of the mineral inclusions in the interface (by SEM–EDS and μ-Raman) revealed that it is mostly constituted of K-feldspars (orthoclase and microcline—$KAlSi_3O_8$) and, in some cases, of diopside crystals ($CaMgSi_2O_6$) as well. Through μ-Raman analysis, mostly orthoclase was identified in the glaze/ceramic interface of the PNS and IVDJ samples, but also microcline, quartz (SiO_2), anatase (TiO_2) and, in sample IVDJ-T 3683, rutile (TiO_2). Wollastonite ($CaSiO_3$), which was widely detected in the SCV samples (Coentro *et al.* 2014), also appears in some PNS samples. When comparing most of the SCV and PNS samples, a Ca-rich layer can be seen in the first ones, but a K-rich interface prevails in the later one, as shown in Figure 6. This is one of the main differences between these collections. In the four IVDJ-S samples analysed by SEM–EDS, both potassium and calcium-rich inclusions show up in the EDS maps. In the three analysed IVDJ-T samples, a K-rich interface appears in all cases.

The presence of diopside indicates firing temperatures above 900 °C, when it is formed, most probably as a reaction product from magnesium-rich minerals, such as dolomite $CaMg(CO_3)_2$ and silicates. The identification of rutile could be an indicator of a still higher firing temperature ($>$1000 °C), but it is known that it could also be related to the raw ceramic material. Therefore, it should not be used here as a temperature marker (Ricciardi 2008).

Synchrotron μ-XRD analysis of the IVDJ samples also identified sanidine crystals in the glaze/ceramic interface (Fig. 4). These crystals can incorporate Pb ions in their structure during firing. The formation of Pb-sanidine crystals is promoted by the high-temperature reaction (800–1000 °C) between lead-rich glazes and potassium-rich ceramic bodies, and has been widely identified in Hispano-Moresque lead glazes (Molera *et al.* 1993; Pradell *et al.* 2010). Lead was also identified in a lead–aluminium silicate ($PbAl_2Si_2O_8$). It is expected that lead reacts with silicates in the glaze and the ceramic body of the tiles, due to the high contents of this element in the glaze composition.

The glaze/ceramic interface in brown glazes consistently shows Ca–Mn-rich inclusions and their acicular shapes suggest the presence of bustamite ($CaMnSi_2O_6$), as identified by μ-Raman in sample PNS07 (Fig. 5 (b)). Bustamite, a Mn-pyroxene, is most probably formed from the reaction between the manganese in the glaze melt and the calcium, mostly from the ceramic paste, at temperatures above 950 °C (Molera *et al.* 2013). Hausmannite (Mn_3O_4), which was identified in SCV samples (Coentro *et al.* 2014) and suggests slightly higher temperatures (~1000 °C) (Molera *et al.* 2013), could not be identified in the collections from Sintra and Spain. Kentrolite ($Pb_2Mn_2Si_2O_9$) was identified in one Spanish sample (the brown glaze in IVDJ 4095—Toledo) (Figs 5 (c) and 5 (d)). It was probably formed through the reaction between the manganese and the silica – lead glaze matrix. The presence of kentrolite suggests lower firing temperatures, since this compound is stable between approximately 650 °C and 840 °C (Molera *et al.* 2013).

CONCLUSIONS

The analysis and comparison of three different collections of Hispano-Moresque glazed tiles revealed a similar technological background for the production of the glazes. Quantitative results obtained by μ-PIXE show similar overall chemical compositions amongst all collections, even when comparing samples from different known provenances, such as the ones from Toledo and from Seville (the IVDJ, Madrid). This is consistent with the existence of a widespread technology in the Iberian Peninsula and its usage in several production centres.

Hispano-Moresque tiles were decorated with high-lead glazes, which were coloured with Cu (green), Co (blue), Mn (brown) and Fe (amber) oxides. White and blue glazes were always opacified with SnO_2, but the other colours appear both with and without tin in their composition —this results in a greater variety of hues (i.e., dark green, light green and turquoise). Such variety is present in PNS and IVDJ samples, but not in the SCV collection. Colorant oxides are completely dissolved in the glaze matrix and few bubbles and inclusions are observed, which suggests that glaze frits were prepared for obtaining the different coloured glazes. The glaze compositions also suggest that two different base recipes were used: one for a tin-opacified glaze and another for a transparent lead glaze, the latter containing more PbO and less SiO_2 and Na_2O in its composition.

In spite of the overall compositional similitude found, the SCV collection differs from the others: it shows higher dispersion in SnO_2 contents (with samples containing >10 wt% SnO_2), higher Fe_2O_3 contents in the amber glaze and a Ca-rich layer in the glaze/ceramic interface. Unfortunately, however, these data are not yet sufficient to confirm or discard a possible local production for this collection. At present, this is as much a valid hypothesis as is the idea that these tiles were imported from a different production centre, either the same as for the Sevillian tiles or a different one.

Adding to this variability, the IVDJ-T glazes are morphologically different from the others, due to the number of inclusions that they contain.

In the PNS collection, the relief tiles show a different glazing technology and have no parallel in the literature. The results suggest a sort of ‘pre-majolica’ technique, with the use of a white tin–lead glaze as a base for all colours, and the pigment and white tin ground concentrations being unevenly distributed, resulting in colour variations. Here, these marked and unique differences strongly suggest a different, possibly local, provenance. These tiles will be the subject of a specific study.

ACKNOWLEDGMENTS

The authors would like to acknowledge Fundação para a Ciência e Tecnologia (FCT) for a Ph.D. grant SFRH/BD/73007/2010 (S. Coentro), a *BI Mestre* grant PTDC/CPC-EAT/4719/2012 (C. Relvas), research project PTDC/CPC-EAT/4719/2012, and research units UID/EAT/00729/2013 and UID/Multi/04349/2013. The authors also acknowledge financial support through LARES (ALENT-07-0224-FEDER-001761) and MICRA.Lab projects (ALENT-07-0262-FEDER-001868) INALENTEJO/QREN/FEDER funding. The authors would also like to thank: Dr Elisa Ramiro and Dr Cristina Partearroyo from the IVDJ, Madrid, for allowing the sampling and for many insightful conversations on Hispano-Moresque tiles; Luis Dias from HERCULES laboratory for the SEM–EDS analysis; Dr Inês Ferro, Dr Joana Amaral and Dr Rita Dargent from the PNS; and Dr Artur Côrte-Real and Dr Catarina Leal from the SCV.

REFERENCES

Barros, 1., Cardoso, G., and Gonçalves, A., 1999, Primeira notícia do forno de S. António da Charneca – Barreiro, *Actas das 3as Jornadas de cerâmica medieval e pós-medieval*, 295–307 (in Portuguese; abstract also in French).

Brill, R. H., 1999, *Chemical analysis of early glasses*, The Corning Museum of Glass, Corning, NY.

Campbell, J. L., Boyd, N. I., Grassi, N., Bonnick, P., and Maxwell, J. A., 2010, The Guelph PIXE software package IV, *Nuclear Instruments and Methods B*, **268**, 3356–63.

Coentro, S., Mimoso, J. M., Lima, A. M., Silva, A. S., Pais, A. N., and Muralha, V. S. F., 2012, Multi-analytical identification of pigments and pigment mixtures used in 17th century Portuguese *azulejos*, *Journal of the European Ceramic Society*, **32**(1), 37–48.

Coentro, S., Trindade, R. A. A., Mirão, J., Candeias, A., Alves, L. C., Silva, R. M. C., and Muralha, V. S. F., 2014, Hispano-Moresque ceramic tiles from the Monastery of Santa Clara-a-Velha (Coimbra, Portugal), *Journal of Archaeological Science*, **41**, 21–8.

Chabanne, D., Bouquillon, A., Aucouturier, M., Dectot, X., and Padeletti, G., 2008, Physico-chemical analyses of Hispano-Moresque lustred ceramic: a precursor for Italian majolica? *Applied Physics A*, **92**(1), 11–18.

Côrte-Real, A., Leal, C., Munhós, M., Macedo, F. P., Bernardo, L., Ferreira, M. A., and Santos, P. C., 2010, O Mosteiro de Santa Clara-a-Velha de Coimbra: investigação, musealização e síntese de aspectos orientalizantes no espólio, in *Actas do IV Congresso de Arqueologia Peninsular: As idades medieval e moderna na Península Ibérica*, 113–28, Faro.

Gratuze, B., Soulier, I., Blet, M., and Vallauri, L., 1997, De lˈorigine du cobalt: du verre à la céramique, *Revue d ˈarchéométrie*, **20**(1), 77–94.

Grime, G. W., and Dawson, M., 1995, Recent developments in data acquisition and processing on the Oxford scanning proton microprobe, *Nuclear Instruments and Methods B*, **104**, 107–13.

Molera, J., Pradell, T., and Vendrell-Saz, M., 1998, The colours of Ca-rich ceramic pastes: origin and characterisation, *Applied Clay Science*, **13**, 187–202.

Molera, J., Vendrell-Saz, M., and Pérez-Arantegui, J., 2001a, Chemical and textural characterization of tin glazes in Islamic ceramics from eastern Spain, *Journal of Archaeological Science*, **28**, 331–40.

Molera, J., Coll, J., Labrador, A., and Pradell, T., 2013, Manganese brown decorations in 10th to 18th century Spanish tin glazed ceramics, *Applied Clay Science*, **82**, 86–90.

Molera, J., Pradell, T., Martinez-Manent, S., and Vendrell-Saz, M., 1993, The growth of sanidine crystals in the lead glazes of Hispano-Moresque pottery, *Applied Clay Science*, **7**, 483–91.

Molera, J., Pradell, T., Salvadó, N., and Vendrell-Saz, M., 2001b, Interactions between clay bodies and lead glazes, *Journal of the American Ceramic Society*, **84**(5), 1120–8.

Molera, J., Pradell, T., Salvadó, N., and Vendrell-Saz, M., 2009, Lead frits in Islamic and Hispano-Moresque glazed productions, in *From mine to microscope: advances in the study of ancient technology* (eds. A. Shortland, I. C. Freestone, and T. Rehren), , ch. 1, 1–0, Oxbow Books, Oxford.

Molera, J., Pradell, T., Merino, L., García-Vallés, M., García-Orellana, J., Salvadó, N., and Vendrell-Saz, M., 1997, La tecnología de la cerámica Islámica y Mudéjar, *Caesaraugusta*, **73**, 15–41.

Mulholland, I. R., 1984, Malayaite and tin-bearing garnet from a skarn at Gumble, NSW, Australia, *Mineralogical Magazine*, **48**, 27–30.

Ortega, L., Cruz Zuluaga, M., Alonso-Olazabal, A., Bienes, J. J., and Solaun, J. L., 2012, Production and technological evolution from Islamic to Christian glazed pottery during 11th to 16th centuries, *Macla*, **16**, 36–7.

Pérez-Arantegui, J., Ortega, J. M., and Escriche, C., 2005, La tecnología de la cerámica Mudéjar entre los siglos XIV y XVI: las producciones esmaltadas de las zonas de Teruel y Zaragoza, in *VI Congreso Ibérico de Arqueometría: avances en arqueometría*, 89–96.

Pérez-Arantegui, J., Ortega, J., and Escriche, C., 2009, The Hispano-Moresque tin glazed ceramics produced in Teruel, Spain: a technology between two historical periods, 13th to 16th c. AD, in *From mine to microscope: advances in the study of ancient technology* (eds. A. Shortland, I. C. Freestone, and T. Rehren), 61–8, Oxbow Books, Oxford.

Pradell, T., Molera, J., Salvadó, N., and Labrador, A., 2010, Synchrotron radiation micro-XRD in the study of glaze technology, *Applied Physics A*, **99**, 407–17.

Ricciardi, P., 2008, *Raman spectroscopy for the non-destructive characterization of ancient pottery, porcelains and mosaic glasses*, Università degli studi di Firenze.

Roldán, C., Coll, J., and Ferrero, J., 2006, EDXRF analysis of blue pigments used in Valencian ceramics from the 14th century to modern times, *Journal of Cultural Heritage*, **7**, 134–8.

RRUFF Project Database, 2014, http://rruff.info/ (accessed 15 December 2014).

Tite, M. S., Maniatis, Y., Kavoussanaki, D., Panagiotaki, M., Shortland, A. J., and Kirk, S. F., 2009, Colour in Minoan faience, *Journal of Archaeological Science*, **36**, 370–8.

Trindade, R. A. A., 2007, *Revestimentos cerâmicos Portugueses: meados do século XIV à primeira metade do século XVI*, Edições Colibri/Faculdade de Ciências Sociais e Humanas da Universidade Nova de Lisboa, Lisboa.

Vendrell-Saz, M., Molera, J., Roqué, J., and Pérez-Arantegui, J., 2006, Islamic and Hispano-Moresque (Múdejar) lead glazes in Spain: a technical approach, in *Geomaterials in cultural heritage* (eds. M. Maggetti and B. Messiga), 163–73, The Geological Society of London, London.

Vieira Ferreira, L. F., Conceição, D. S., Ferreira, D. P., Santos, L. F., Casimiro, T. M., and Ferreira Machado, I., 2014, Portuguese 16th century tiles from Santo António da Charneca's kiln: a spectroscopic characterization of pigments, glazes and pastes, *Journal of Raman Spectroscopy*, **45**, 838–47.

Zucchiatti, A., Bouquillon, A., Katona, I., and D'Alessandro, A., 2006, The 'Della Robbia blue': a case study for the use of cobalt pigments in ceramics during the Italian Renaissance, *Archaeometry*, **48**, 131–52.

SUPPORTING INFORMATION

Additional Supporting Information may be found in the online version of this paper at the publisher's web-site:

Table S1. Chemical composition (in wt.%) of the analysed tiles from PNS, SCV and IVDJ collections, obtained by μ-PIXE. Results are divided by colour. Techniques: A arista, CS cuerda seca, R relief, F flat.

Figure S1. Samples from each studied collection.